Solid State Sciences 17 (2013) 97–101

Contents lists available at SciVerse ScienceDirect

Solid State Sciences

journal homepage: www.elsevier.com/locate/ssscie

# Magnetic characteristics of nanocrystalline GaMnN films deposited by reactive sputtering

D.M.G. Leite [a,*], A.L.J. Pereira [a], W.A. Iwamoto [b], P.G. Pagliuso [b], P.N. Lisboa-Filho [a], J.H.D. da Silva [a]

[a] Advanced Materials Group, UNESP – Univ Estadual Paulista, Bauru 17033-360, SP, Brazil
[b] Instituto de Física "Gleb Wataghin", Unicamp, Campinas 13083-970, SP, Brazil

ARTICLE INFO

*Article history:*
Received 16 April 2012
Received in revised form
14 November 2012
Accepted 25 November 2012
Available online 4 December 2012

*Keywords:*
Sputtering
GaMnN
Nanocrystalline material
Diluted magnetic semiconductor
Magnetic properties

ABSTRACT

The magnetic characteristics of $Ga_{1-x}Mn_xN$ nanocrystalline films ($x = 0.08$ and $x = 0.18$), grown by reactive sputtering onto amorphous silica substrates (a-$SiO_2$), are shown. Further than the dominant paramagnetic-like behaviour, both field- and temperature-dependent magnetization curves presented some particular features indicating the presence of secondary magnetic phases. A simple and qualitative analysis based on the Brillouin function assisted the interpretation of these secondary magnetic contributions, which were tentatively attributed to antiferromagnetic and ferromagnetic phases.



## 1. Introduction

Diluted magnetic semiconductors (DMS) have attracted the attention of several research groups due to their potential for fabrication of functional spintronic devices [1–3]. In particular, $Ga_{1-x}Mn_xN$ is expected – once doped with a sufficient amount of free or weakly localized holes – to show ferromagnetism at room temperature, a critical requirement for practical applications [1–3]. To date, numerous experiments have demonstrated that $Ga_{1-x}Mn_xN$ systems can show ferromagnetism (FM) [4,5], paramagnetism (PM) [6,7], antiferromagnetism (AFM) [8,9] and superparamagnetism (SPM) [10], as a function mainly of the Mn concentration and the microstructure of the sublattice (GaN).

In selected monocrystalline GaMnN samples, where the incorporated Mn is believed to be diluted, either pure paramagnetism [6,7] or room temperature ferromagnetism [4,5] can be found. In this case, the Mn concentration plays a major role: for samples containing up to 1% of diluted Mn ($x = 0.01$), only paramagnetic phase is detected for temperatures from 1.8 to 300 K [6,7], while for Mn concentrations above 3% ($x = 0.03$), a ferromagnetic phase is reported [4] at up to 940 K [5]. However, no consensus has yet been reached about the microscopic mechanisms that give rise to the ferromagnetic phase in monocrystalline GaMnN. Two main approaches have been considered in the literature: the direct double exchange mechanism [11,12] and the carrier mediated Zener model [1,2].

The discussion becomes more complicated when considering nanocrystalline GaMnN systems. In these cases, the presence of a significant portion of disorder – mainly represented by the presence of grain boundaries – gives rise to different geometric and chemical environments for the Mn sites, beyond those expected in a well-organized monocrystalline GaN matrix. This complex situation leads to new possibilities with respect to the magnetic interaction between the Mn ions, even if they are present in a diluted regime. In fact, antiferromagnetism [8,9] and superparamagnetism [10] are commonly reported for nanocrystalline $Ga_{1-x}Mn_xN$ with a variety of Mn concentrations up to 18% ($x = 0.18$). The antiferromagnetism is especially attributed to the presence of a significant portion of $Mn^{2+}$ ($d^5$) instead of the expected $Mn^{3+}$ ($d^4$). Furthermore, it is also reasonable to consider the possibility of coexisting magnetic phases in nanocrystalline GaMnN systems. In this case, the results from superconductor quantum interference device (SQUID) magnetometry become quite difficult to interpret, which leads, in most cases, to incomplete or even incorrect conclusions about the real magnetic phases present in this type of material.

* Corresponding author. Departamento de Física, Univ. Estadual Paulista – UNESP, Av. Eng. Edmundo C. Coube, 14-01, CEP 17033-360 Bauru, SP, Brazil. Tel.: +55 (14) 3103 6178; fax: +55 (14) 3103 6084.
*E-mail address:* dmgleite@fc.unesp.br (D.M.G. Leite).

1293-2558/$ – see front matter © 2012 Elsevier Masson SAS. All rights reserved.
http://dx.doi.org/10.1016/j.solidstatesciences.2012.11.020

In this work, we report a systematic magnetic characterization and analysis of $Ga_{1-x}Mn_xN$ nanocrystalline films ($x = 0.08$ and $x = 0.18$) grown by reactive sputtering onto amorphous silica substrates (a-$SiO_2$) [13–17]. A simple and qualitative analysis based on the Brillouin function indicate the presence of secondary magnetic contributions tentatively attributed to antiferromagnetic and ferromagnetic phases further than the dominant paramagnetic contribution from non-interacting Mn ions.

## 2. Experimental details

$Ga_{1-x}Mn_xN$ nanocrystalline films ($x = 0.08$ and 0.18) were grown by reactive sputtering onto amorphous silica (a-$SiO_2$) at relatively low substrate temperature ($T_S \sim 200$ °C) [13–17]. Only α-GaN (wurtzite) phase could be identified by X-ray diffraction (XRD). High-resolution transmission electron microscopy (HRTEM) and electron diffraction measurements showed that the films treated here are composed of a thin intermediate layer of non-oriented nanocrystals (diameter ~5 nm) and a posterior columnar structure (diameter ~30 nm) that is highly oriented with <0001> direction perpendicular to the film surface [17]. The thickness of the intermediate layer was around 50 nm for $x = 0.08$ and around 65 nm for $x = 0.18$ sample – the total film thicknesses were 900 nm and 640 nm, respectively. Despite the nanostructure of these films, Energy Filtered TEM measurements performed on $x = 0.18$ sample showed no evidence of Mn segregation up to the achieved resolution (5 nm) [17]. It is important to mention that the samples were not intentionally codoped and all the extrinsic carriers probably present should be related to: (i) Mn incorporation in different charge states and (ii) all the possible defects such as vacancies and crystallites surface states.

For the magnetic characterization, selected samples were cut in approximately 5 × 10 mm geometry. In order to avoid any kind of magnetic contamination, special care was taken with the sample manipulation including the use of plastic tweezers only, the use of previously tested diamagnetic plastic tubes to contain the samples, and systematic tests with pure substrates. These precautions are strictly necessary due to the very low magnetic moments of the samples and the high sensitivity of the SQUID magnetometer, as pointed out by other groups [18].

The magnetic characterization was performed in a SQUID magnetometer using field-dependent magnetization loops with applied magnetic field from −50 to 50 kOe taken at temperatures from 2 to 300 K; and temperature-dependent magnetization curves using zero field cooled (ZFC) and field cooled (FC) loops under applied magnetic field from 0.1 to 10 kOe. All magnetic measurements shown here were performed in the DC configuration with an applied field parallel to the sample surface (in-plane field). Each magnetization point was obtained as the arithmetic average of two sample excursions through the SQUID coils, with each excursion 12 cm long and divided into 25 points.

## 3. Results

Fig. 1(a) shows the in-plane total magnetization curves for $x = 0.08$ and $x = 0.18$ $Ga_{1-x}Mn_xN$ samples taken at 2 and 300 K. The a-$SiO_2$ substrate magnetization curve taken at 2 K was added for comparison: the same response is obtained at 300 K, which indicates pure diamagnetic behaviour. In Fig. 1(a), the total magnetization has been simply determined using the total mass (film + substrate) of each sample. In Fig. 1(b), the substrate diamagnetism has been appropriately subtracted from the GaMnN samples and the magnetization was now determined by the film volume of the $x = 0.08$ and $x = 0.18$ samples ($4.94 \times 10^{-5}$ $cm^3$ and $1.66 \times 10^{-5}$ $cm^3$, respectively).

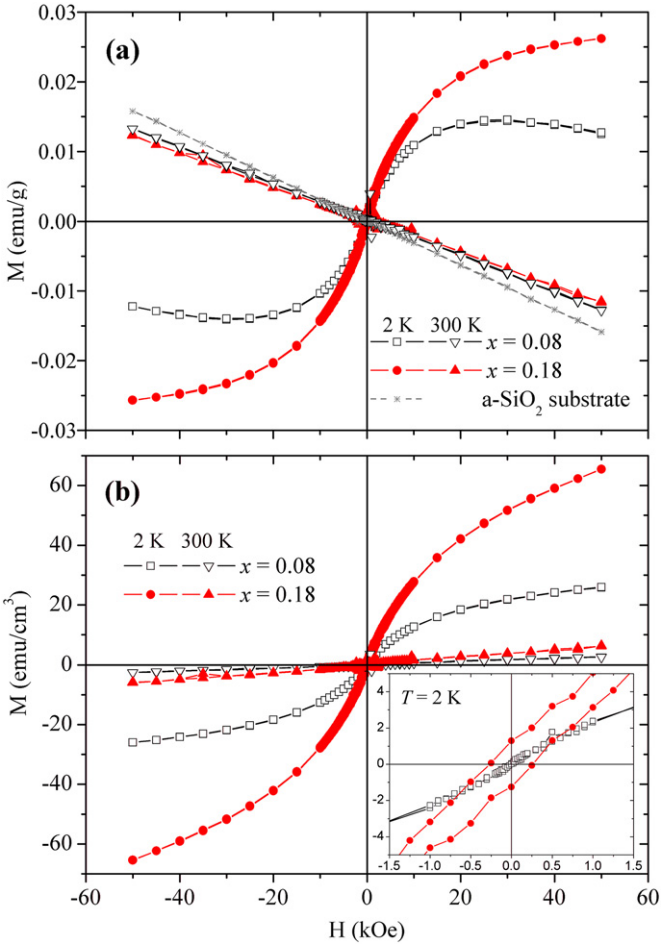


**Fig. 1.** (a) Total magnetization curves for $x = 0.08$ and $x = 0.18$ $Ga_{1-x}Mn_xN$ samples taken at 2 K and 300 K. The magnetization of a pure a-$SiO_2$ substrate taken at 2 K was added for comparison. The total mass of each sample was used to determine the total magnetization in emu/g. (b) Corrected magnetization curves obtained by subtracting the substrate diamagnetism and using the respective film volume to determine the magnetization in emu/$cm^3$.

After the correction, the magnetization curves in Fig. 1(b) and in all of the following graphs can be, in a first approximation, directly related to the presence of Mn ions in the samples. This is due to the fact that our pure GaN sample ($x = 0.00$) been purely diamagnetic with practically the same susceptibility as the pure a-$SiO_2$ substrate, furthermore, no magnetic anisotropy was observed by performing in-plane and out-of-plane measurements.

Despite of the fact that *M vs H* curves show typical paramagnetic characteristics: smooth S-shape at low temperatures ($T < 50$ K) and a linear shape with weak positive susceptibility at higher temperatures ($T > 100$ K); two remarks should be emphasised: (i) the presence of a weak hysteresis loop at $T = 2$ K for the sample with highest Mn content ($x = 0.18$) shown in the inset of Fig. 1(b); and (ii) a quasi-linear increase of the magnetization for $H > 20$ kOe for $T = 2$ K for both samples (Fig. 1(b)). Both features indicate that secondary magnetic phases, further than an ordinary paramagnetic phase, are contributing to the total magnetization of the studied samples. In fact, the tentative of describing our experimental *M vs H* curves at $T < 50$ K with a unique Brillouin function (Equation (1)) just fails.

For this reason, and in order to get a better but still qualitative insight into the possible magnetic phases present, the following procedure, based on the use of multiple Brillouin functions and supported by recent literature [2,8,9], is adopted here. In the